Complex formation and water exchange on the trinuclear dioxo-capped complexes [M3(μ3-O)2(μ-CH3CO 2)6(OH2)3]2+ (M = Mo, W) and monooxo-capped complex [W3(μ3-O)(μ-CH3CO2) 6(OH2)3]2+

ARTICLE *in* INORGANIC CHEMISTRY · SEPTEMBER 1993

Impact Factor: 4.76 · DOI: 10.1021/ic00071a010

Complex Formation and Water Exchange on the Trinuclear Dioxo-Capped Complexes $[M_3(\mu_3\text{-}O)_2(\mu\text{-}CH_3CO_2)_6(OH_2)_3]^{2+}$ (M = Mo, W) and Monooxo-Capped Complex $[W_3(\mu_3\text{-}O)(\mu\text{-}CH_3CO_2)_6(OH_2)_3]^{2+}$

Glenmore Powell and David T. Richens*

Chemistry Department, University of St. Andrews, North Haugh, St. Andrews, Fife KY16 9ST, Scotland, U.K.

Received March 23, 1993

Kinetic studies of complex formation and water exchange carried out in aqueous solution, I = 1.0 M ($NaCF_3SO_3$), on the trinuclear dioxo-capped acetato-bridged complexes $[M_3(\mu_3\text{-}O)_2(\mu\text{-}CH_3CO_2)_6(OH_2)_3]^{2+}$ (M = Mo, W) and monooxo-capped complex $[W_3(\mu_3\text{-}O)(\mu\text{-}CH_3CO_2)_6(OH_2)_3]^{2+}$ are reported. Comparisons of kinetic data for NCS^-, $C_2O_4^{2-}$, and CD_3OD complexation with that for water exchange suggest an I_d mechanism for reactions occurring on $[Mo_3(\mu_3\text{-}O)_2(\mu\text{-}CH_3CO_2)_6(OH_2)_3]^{2+}$. Substitution of water by $HC_2O_4^-$ on $[Mo_3(\mu_3\text{-}O)_2(\mu\text{-}CH_3CO_2)_6(OH_2)_3]^{2+}$ takes place by a concerted mechanism wherein the outgoing water ligand derives from C–O bond breakage. Extremely low $\Delta H^{\ddagger}$ (53, 58 kJ mol^{-1}) and markedly negative $\Delta S^{\ddagger}$ (−130, −164 J K^{-1} mol^{-1}) values characterize water exchange respectively on the monooxo- and dioxo-capped tungsten complexes, implying the presence of a unique changeover in water exchange mechanism, I_d(Mo) to I_a(W), in these complexes. For $[W_3(\mu_3\text{-}O)(\mu\text{-}CH_3CO_2)_6(OH_2)_3]^{2+}$ a water exchange rate constant (25 °C) 100× larger than that on $[Mo_3(\mu_3\text{-}O)_2(\mu\text{-}CH_3CO_2)_6(OH_2)_3]^{2+}$ is observed. The results from complex formation studies on the two tungsten complexes suggests that the mechanistic changeover may be unique to the water exchange process.

Trinuclear acetato-bridged cluster complexes $[M_3(\mu_3\text{-}X)_n(CH_3CO_2)_6L_3]^{m+}$ are now well characterized for a number of the early transition metals,[1] namely niobium (X = O, n = 2, L = THF, m = 1),[2] molybdenum (X = O or CCH_3, n = 2, L = H_2O or pyridine, m = 1 or 2),[3-8] and tungsten (X = O, n = 1 or 2, L = H_2O, m = 2).[9-12] In the case of molybdenum several of the complexes were first "synthesised" some 29 years ago following reactions of $Mo(CO)_6$ with acetic acid from which the first quadruply-bonded dimolybdenum(II) complex. $Mo_2(CH_3CO_2)_4$, was isolated. However suspicions were aroused of the existence of additional or alternative products during unsuccessful attempts to make the corresponding ditungsten(II) tetraacetate complex using $W(CO)_6$.[9] Finally in 1976 the accompanying formation of triangular acetato-bridged clusters in these reactions was established.[3] Since then much progress has been made in understanding these reactions,[13] and it is now recognized that these elements have a marked tendency to form triangular clusters in mean formal oxidation state (III–IV).[1,14-17] Examples include M_3X_{13} species, wherein the M(IV) "aqua ions" $[M_3(\mu_3\text{-}X)(\mu\text{-}X)_3(OH_2)_9]^{4+}$ (M = Mo or W; X = O or S)[18-20] are prototypal examples, and the oxo-capped bridged-alkoxide complexes such as $[Mo_3(\mu_3\text{-}O)(\mu\text{-}OR)(\mu\text{-}OR)_3(OR)_6]$ extensively studied by Chisholm.[21,22] For the dioxo-capped complexes the basis structural unit (I) has now been established by a number of X-ray structures for both Mo and W compounds.[3-12] Mixed Mo_2W and MoW_2 species have also been structurally characterized.[23] Interestingly the monooxo-capped 8e⁻ structure (II) is only known for tungsten although a 10e⁻ structure for molybdenum with a single μ-oxo cap has been recently reported.[24]

In the case of the triangular $[M_3(\mu_3\text{-}X)(\mu\text{-}X)_3(OH_2)_9]^{4+}$ "aqua" ions (M = Mo or W) a number of recent kinetic studies have helped to elucidate the mechanism of terminal water ligand replacement.[18,25-29] Within these species two kinds of terminal water ligand are present with those (d-type) trans to the bridging-X ligands (two per M) more labile by a factor of 10^5 than those (c-type) trans to the capping μ_3-X ligand (one per M). The lability in the d-type H_2O's arises via cis-conjugate base activation through a monohydroxy form (deprotonation on the same metal).[25] There

(1) Cotton, F. A. *Polyhedron* **1986**, *5*, 3–14 and references therein.
(2) Cotton, F. A.; Diebold, M. P.; Roth, W. J. *Inorg. Chem.* **1988**, *27*, 2347.
(3) Bino, A.; Ardon, M.; Maor, I.; Kaftory, M.; Dori, Z. *J. Am. Chem. Soc.* **1976**, *98*, 7093.
(4) Bino, A.; Cotton, F. A.; Dori, Z. *J. Am. Chem. Soc.* **1981**, *103*, 243.
(5) Ardon, M.; Bino, A.; Cotton, F. A.; Dori, Z.; Kaftory, M.; Reisner, G. M. *Inorg. Chem.* **1982**, *21*, 1912.
(6) Ardon, M.; Bino, A.; Cotton, F. A.; Dori, Z.; Kaftory, M.; Kolthammer, B. W. S.; Kapon, M.; Reisner, G. M. *Inorg. Chem.* **1981**, *20*, 4083.
(7) Bino, A.; Cotton, F. A.; Dori, Z.; Falvello, L. R.; Reisner, G. M. *Inorg. Chem.* **1982**, *21*, 3750.
(8) Bino, A.; Gibson, D. *Inorg. Chim. Acta* **1982**, *65*, L37.
(9) Bino, A.; Cotton, F. A.; Dori, Z.; Koch, S.; Kuppers, H.; Miller, M.; Sekutowski, J. C. *Inorg. Chem.* **1978**, *17*, 3245.
(10) Cotton, F. A.; Dori, Z.; Kapon, M.; Marler, D. O.; Reisner, G. M.; Schwotzer, W.; Shaia, M. *Inorg. Chem.* **1985**, *24*, 4381.
(11) Ardon, M.; Cotton, F. A.; Dori, Z.; Fang, A.; Kapon, M.; Reisner, G. M.; Shaia, M. *J. Am. Chem. Soc.* **1982**, *104*, 5394.
(12) Bino, A.; Cotton, F. A.; Dori, Z.; Shaia-Gottlieb, M.; Kapon, M. *Inorg. Chem.* **1988**, *27*, 3592.
(13) Bino, A.; Cotton, F. A.; Dori, Z.; Kolthammer, B. W. S. *J. Am. Chem. Soc.* **1981**, *103*, 5779.
(14) Muller, A.; Jostes, R.; Cotton, F. A. *Angew. Chem., Int. Ed. Engl.* **1980**, *19*, 875.
(15) Wendan, C.; Qianer, Z.; Jinshun, H.; Jiaxi, L. *Polyhedron* **1989**, *8*, 2785.
(16) Bursten, B. E.; Cotton, F. A.; Hall, M. B.; Najjar, R. C. *Inorg. Chem.* **1982**, *21*, 302.
(17) Cotton, F. A.; Shang, M.; Sheng Sun, Z. *J. Am. Chem. Soc.* **1991**, *113*, 3007.
(18) Richens, D. T.; Helm, L.; Pittet, P.-A.; Merbach, A. E.; Nicolo, F.; Chapuis, G. *Inorg. Chem.* **1989**, *28*, 1394.
(19) Akashi, H.; Shibahara, T.; Kuroya, H. *Polyhedron* **1990**, *9*, 1671.
(20) Shibahara, T.; Takeuchi, A.; Ohtsuji, A.; Kohda, K.; Kuroya, H. *Inorg. Chim. Acta* **1987**, *127*, L45.
(21) Chisholm, M. H.; Folting, K.; Huffman, J. C.; Kirkpatrick, C. C. *J. Am. Chem. Soc.* **1981**, *103*, 5967.
(22) Chisholm, M. H.; Cotton, F. A.; Fang, A.; Kober, E. M. *Inorg. Chem.* **1984**, *23*, 749.
(23) Wang, B.; Sasaki, Y.; Nagasawa, A.; Ito, T. *J. Am. Chem. Soc.* **1986**, *108*, 6059. and *J. Cord. Chem.* **1988**, *18*, 45.
(24) Li, X.; Jinshun, H.; Qianer, Z. Private communication, 1992.
(25) Richens, D. T.; Pittet, P.-A.; Merbach, A. E.; Humanes, M.; Lamprecht, G. J.; Ooi, B.-L.; Sykes, A. G. *J. Chem. Soc., Dalton Trans.*, in press.
(26) Ooi, B.-L.; Sykes, A. G. *Inorg. Chem.* **1988**, *27*, 310; **1989**, *28*, 3799.
(27) Ooi, B.-L.; Petrou, A.; Sykes, A. G. *Inorg. Chem.* **1988**, *27*, 3626.
(28) Routledge, C. A.; Sykes, A. G. *J. Chem. Soc., Dalton Trans.* **1992**, 325.
(29) Rodgers, K. R.; Murmann, R. K.; Schlemper, E. O.; Shelton, M. E. *Inorg. Chem.* **1985**, *24*, 1313.

0020-1669/93/1332-4021$04.00/0

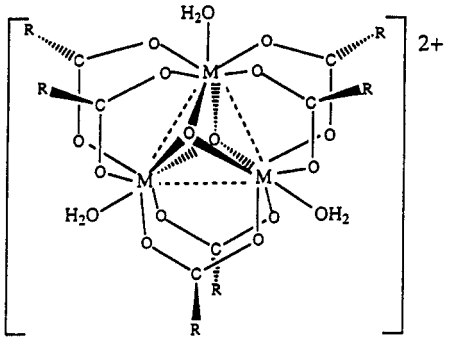

(I)

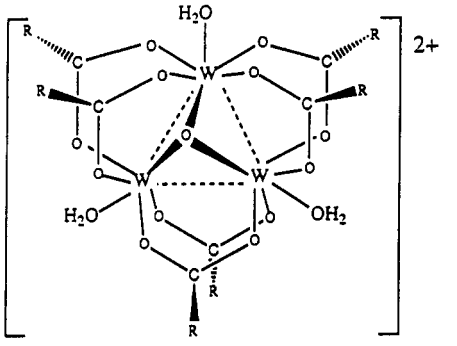

(II)

have been few kinetic studies of complexation/exchange reactions at the terminal L ligands carried out on the corresponding triangular acetato-bridged clusters of Mo^{IV} and W^{IV} for comparison. Such studies would be of interest for several reasons. First, the acetato-bridged clusters have no possibility of cis-conjugate base activation since they possess only one terminal H_2O ligand on each metal center. Second, a comparison of bridging group μ-$CH_3CO_2^-$ versus μ-O^{2-} or μ-S^{2-} could be carried out, and third a comparison of lower overall cluster charge 2+ versus 4+ would be possible. Moreover, this family of clusters offers a rare opportunity, for the dioxo-capped species, to compare the behavior of W versus Mo within the same type of compound and, for M = W, the effect of only one capping μ-oxo ligand in addition to a different oxidation state $M^{III}_2M^{IV}$ versus M^{IV}_3. Sasaki et al. have reported kinetic studies of terminal water replacement by CD_3OD on $[Mo_3(\mu_3\text{-}X)_2(CH_3CO_2)_6(OH_2)_3]^{n+}$ carried out using ^1H NMR in pure CD_3OD.[30] They detected a significant trans labilizing effect (factor of 10^5) for $X = CCH_3^{3-}$ ($n = 1$) versus $X = O^{2-}$ ($n = 2$). No kinetic studies appear to have been previously carried out on any of these complexes in aqueous solution.

We wish to report here the results of kinetic studies carried out on $[M_3(\mu_3\text{-}O)_n(\mu\text{-}CH_3CO_2)_6(OH_2)_3]^{2+}$ with regard to water exchange ($n = 2$, M = Mo, W; $n = 1$, M = W) and complex formation by NCS^- ($n = 2$, M = Mo; $n = 1$, M = W), and oxalate ($n = 2$, M = Mo, W) in noncomplexing aqueous media, I = 1.0 M ($CF_3SO_3^-$). Some intriguing conclusions are made regarding the mechanisms of reactions occurring on W versus Mo in these compounds.

Experimental Section

Preparation of Complexes. (a) Hexakis(μ-acetato)triaquabis(μ_3-oxo)trimolybdenum(IV) Perchlorate, $[Mo_3(\mu_3\text{-}O)_2(\mu\text{-}CH_3CO_2)_6(OH_2)_3](ClO_4)_2$. Two methods have now been devised for the preparation of this complex. In method A, $Mo(CO)_6$ (Merck) (1.0 g) was refluxed in a 1:1 mixture of acetic acid and acetic anhydride (100 cm^3) under a stream of O_2 for between 24 and 36 h.[4] Following cooling and dilution five times with water, the resulting solution was chromatographed on a 10 cm × 2 cm column of Dowex 50W-X2 cation-exchange resin (H^+ form) from which, following washing with water and 0.01 M $HClO_4$, the desired complex could be eluted as a bright red band with 0.5M $HClO_4$. Slow evaporation of the eluates yielded pinkish-red crystals of the bis(perchlorate) salt. In method B a mixture of recrystallized sodium molybdate dihydrate (2.0 g) and $W(CO)_6$ (Merck) (4.0 g) was refluxed under N_2 in acetic anhydride (200 cm^3) for 5 h.[31] The solution was filtered and the solid obtained was dissolved in water, producing a reddish orange solution. Following further filtration to remove undissolved solid, the resulting solution was then chromatographed as in method A. In this case two species could be observed on the column and were successively eluted with 0.5 M $HClO_4$. The first red band contained $[Mo_3O_2(CH_3CO_2)_6(OH_2)_3]^{2+}$. The second band was orange and subsequently shown to contain the mixed Mo–W complex $[MoW_2O_2(CH_3CO_2)_6(OH_2)_3]^{2+}$. A small amount of the Mo_2W cluster was also found in solid samples of the MoW_2 cluster by ^1H NMR in D_2O. $[Mo_3(\mu_3\text{-}O)_2(\mu\text{-}CH_3CO_2)_6(OH_2)_3](ClO_4)_2$ was characterized by its UV–visible spectrum in 1.0 M $HClO_4$, λ_{max} at 505 nm (ϵ = 700 M^{-1} cm^{-1} per Mo_3) and 430 nm (500)[23] and by its ^1H NMR spectrum in D_2O (singlet (18H) at 1.61 ppm from TMS).[23] A fast atom bombardment mass spectrum of $[Mo_3(\mu_3\text{-}O)_2(\mu\text{-}CH_3CO_2)_6(OH_2)_3](ClO_4)_2$ in a nitrobenzyl alcohol matrix showed an M^{*+} peak at 729 and a fragmentation pattern showing successive loss of the three terminal water ligands.

(b) Hexakis(μ-acetato)triaquabis(μ_3-oxo)tritungsten(IV) Perchlorate, $[W_3(\mu_3\text{-}O)_2(\mu\text{-}CH_3CO_2)_6(OH_2)_3](ClO_4)_2$. $W(CO)_6$ (1.0 g) was refluxed in a 1:1 mixture of acetic acid and acetic anhydride (100 cm^3) for 12 h.[9] The mixture was cooled and the resulting yellow precipitate filtered off. The filtrate was diluted with water (100 cm^3) and passed down a 20 cm × 2 cm column of Dowex 50W-X2 cation-exchange resin (H^+ form). A bright greenish-yellow band was absorbed and, following washing of the column with water, was eluted with 1.0M $HClO_4$. Yellow crystals of the title complex were obtained by slow evaporation. The complex was characterized by its UV–visible spectrum in 1.0 M $HClO_4$. λ_{max} = 445 nm (ϵ = 2300 M^{-1} cm^{-1} per W_3) and 350 nm (1500)[23] and by its ^1H NMR spectrum in D_2O (singlet (18H) at 1.71 ppm from TMS).[23] Microanalyses on a sample of the yellow solid gave 12.00% C and 2.24% H. $[W_3(\mu_3\text{-}O)_2(\mu\text{-}CH_3CO_2)_6(OH_2)_3](ClO_4)_2\cdot 1.5H_2O$ $C_{12}H_{27}O_{26.5}Cl_2W_3$ requires 11.82% C and 2.22% H.

(c) Hexakis(μ-acetato)triaqua(μ_3-oxo)tritungsten(III,III,IV) Perchlorate, $[W_3(\mu_3\text{-}O)(\mu\text{-}CH_3CO_2)_6(OH_2)_3](ClO_4)_2$. This complex was prepared by refluxing a mixture of sodium tungstate hydrate (5.0 g) and granulated zinc (5.0 g) in acetic anhydride (60cm^3) for 10 h.[12] When the mixture was cooled to room temperature, a greenish yellow precipitate was formed, which was filtered and washed with ethanol and diethyl ether. The solid was dissolved in water and, following filtration, the resulting solution was passed down a 20cm × 2cm column of Dowex 50W-X2 cation-exchange resin which retained a blue band while allowing a yellow solution to pass through. The yellow solution contained the dioxo-capped anion $[W_3(\mu_3\text{-}O)_2(\mu\text{-}CH_3CO_2)_6(CH_3CO_2)_3]^-$. Following washing with water, to remove the last traces of the yellow anion, the blue band was eluted with 1.0 M $HClO_4$. Crystals of the title complex were obtained by slow evaporation of the eluate as before. Crystals of the triflate salt were subsequently obtained by elution from the column with 2.0 M CF_3SO_3H and slow evaporation. The complex was characterized by its UV–visible spectrum in 1.0 M $HClO_4$, which agreed well with the published values, λ_{max} at 668 nm (ϵ = 1245 M^{-1} cm^{-1} per W_3), 508 (625), 404 (1016), and 340 (2375).[11]

Figure 1 shows electronic spectra recorded in 1.0 M $HClO_4$ for the bis(μ_3-oxo)-capped complexes $[M_3(\mu_3\text{-}O)_2(\mu\text{-}CH_3CO_2)_6(OH_2)_3]^{2+}$ (M_3 = Mo_3 and W_3).

Kinetic Studies. (a) Complex Formation Reactions on $[Mo_3(\mu_3\text{-}O)_2(\mu\text{-}CH_3CO_2)_6(OH_2)_3]^{2+}$. (i) NCS^-. This study was carried out using a large excess of NCS^- (0.1–0.9 M) over complex ($\sim 4 \times 10^{-4}$ M) at I = 1.0 M ($NaCF_3SO_3$), pH 3.0, and temperature range 47–60 °C. Figure 2 shows scan spectra taken at 1-h intervals at 47 °C, pH 3.0. Substitution of terminal H_2O by NCS^- is accompanied by a marked rise in absorbance below 440 nm due to the appearance of an intense $NCS^- \rightarrow$ Mo charge transfer band. The complexation reaction was monitored at 400 nm.

(ii) Oxalate. The study was again carried out using an excess of oxalate (0.01–0.05 M) over complex ($\sim 2 \times 10^{-4}$ M) in the pH range 2.54–3.89 at I = 1.0 M ($NaCF_3SO_3$), range 40–55 °C. The lower oxalate concentrations used in this study were as a result of the low solubility of

(30) Nakata, K.; Nagasawa, A.; Soyama, N.; Sasaki, Y.; Ito, T. *Inorg. Chem.* **1991**, *30*, 1575.

(31) Birnbaum, A.; Cotton, F. A.; Dori, Z.; Marler, D. O.; Reisner, G. M.; Schwotzer, W.; Shaia, M. *Inorg. Chem.* **1983**, *22*, 2723.

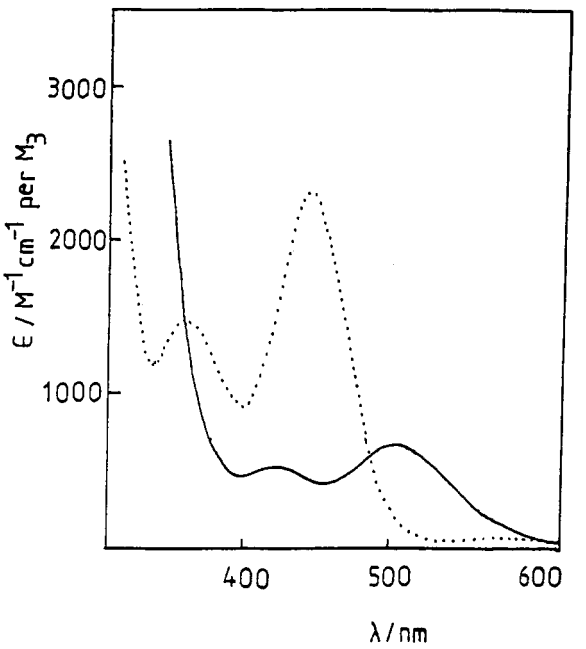

Figure 1. Electronic spectra of $[M_3(\mu_3\text{-}O)_2(\mu\text{-}CH_3CO_2)_6(OH_2)_3]^{2+}$ complexes in 1.0 M $HClO_4$: (—) Mo; (···) W.

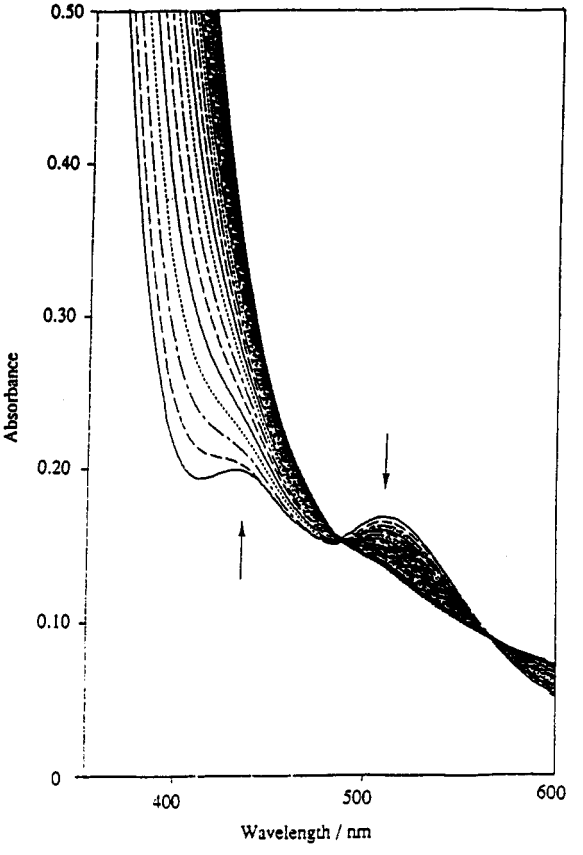

Figure 2. Changes to the electronic spectrum of $[Mo_3(\mu_3\text{-}O)_2(\mu\text{-}CH_3CO_2)_6(OH_2)_3]^{2+}$ ($\sim 4 \times 10^{-4}$ M) during reaction with NCS^- (0.9 M) at 47 °C, pH 3.0, and I = 1.0 M ($NaCF_3SO_3$). Time interval between spectra = 1 h.

oxalate at I = 1.0 M. In this case absorbance changes were much smaller in the visible region, Figure 3, and so the reaction was monitored at 340 nm.

(b) Complex Formation Reactions on $[W_3(\mu_3\text{-}O)_2(\mu\text{-}CH_3CO_2)_6(OH_2)_3]^{2+}$. Oxalate. This reaction was monitored at 340 nm with an excess of oxalate (0.01–0.05 M) over complex ($\sim 1 \times 10^{-4}$ M) at 55 °C, pH 3.83, and I = 1.0 M ($NaCF_3SO_3$). It was necessary to deoxygenate the run solutions because of the inherent air-sensitivity of the tungsten complexes over the prolonged reaction times at these temperatures.

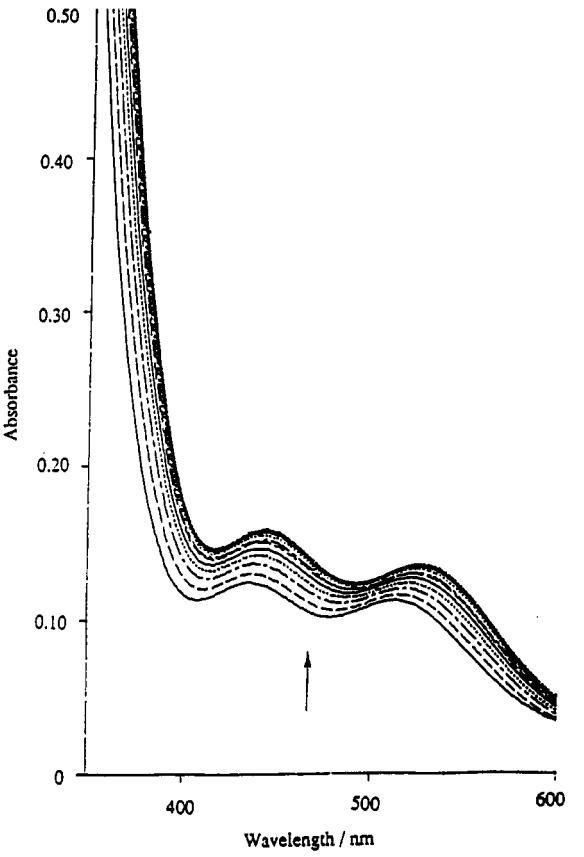

Figure 3. Changes to the electronic spectrum of $[Mo_3(\mu_3\text{-}O)_2(\mu\text{-}CH_3CO_2)_6(OH_2)_3]^{2+}$ ($\sim 2 \times 10^{-4}$ M) during reaction with oxalate (0.01 M) at 47 °C, pH 3.2, and I = 1.0 M ($NaCF_3SO_3$). Time interval between spectra = 20 min.

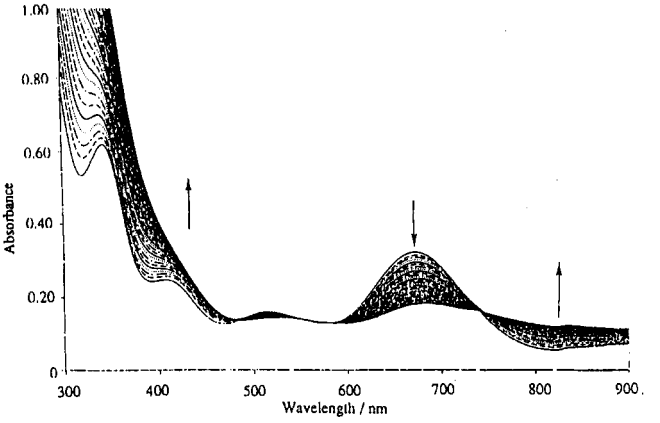

Figure 4. Changes to the electronic spectrum of $[W_3(\mu_3\text{-}O)(\mu\text{-}CH_3CO_2)_6(OH_2)_3]^{2+}$ (2.5×10^{-4} M) during reaction with NCS^- (0.2 M) at 50 °C, pH 2.0, and I = 1.0 M ($NaCF_3SO_3$). Time interval between spectra = 30 min.

(c) Complex Formation Reactions on $[W_3(\mu_3\text{-}O)(\mu\text{-}CH_3CO_2)_6(OH_2)_3]^{2+}$. NCS^-. For this study a large excess of NCS^- (0.2–0.95 M) over complex ($\sim$(1–3) $\times 10^{-4}$ M) was used at pH 2.0, 50 °C, and I = 1.0 M ($NaCF_3SO_3$). Runs were conducted under air-free conditions as for the bicapped W complex. The absorbance changes consisted of a decrease in the peak maximum at 686 nm coupled with a rise in absorbance above 730 nm and below 480 nm. Figure 4 shows typical spectral changes observed for a run with NCS^- (0.2 M) and complex (2.5×10^{-4} M). The appearance of an intense $NCS^- \rightarrow$ M charge transfer band was again evident below 430 nm and the reaction was conveniently monitored at 400 nm.

Instrumentation. UV–visible spectra and fixed wavelength kinetics were recorded in 1-cm quartz cuvettes using a Perkin-Elmer Lambda 5 spectrophotometer with electronic thermostating (±0.1 °C) and auto cell change facilities. A Radiometer PHM82 pH meter was used with a Russell CWR/320/757 narrow stem combination glass/Ag/AgCl

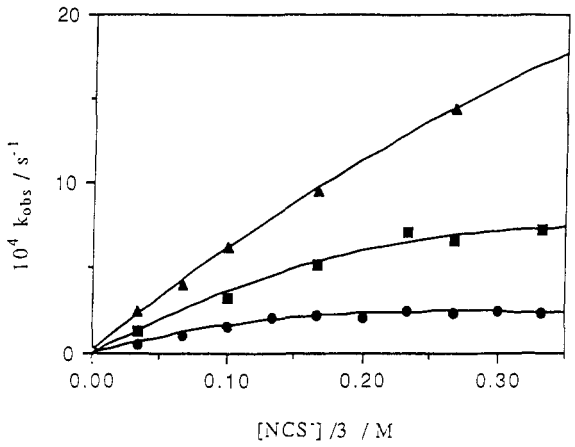

Figure 5. Plots of k_{obs} (s^{-1}) versus [NCS^-]/3 (M) for the first stage of reaction of $[Mo_3(\mu_3\text{-}O)_2(\mu\text{-}CH_3CO_2)_6(OH_2)_3]^{2+}$ with NCS; pH 3.0, I = 1.0 M ($NaCF_3SO_3$); (●) 47 °C; (■) 55 °C; (▲) 60 °C.

electrode, which allowed direct pH measurement inside the 1-cm cuvettes. The pH meter was calibrated with solutions at pH 2 and 4 at I = 1.0 M ($NaCF_3SO_3$).

Kinetics of Water Exchange. This was studied by ^{17}O NMR following addition of solid complex to 2 cm^3 samples containing 10 atom % H_2O^{17} (Yeda, Israel) at I = 1.0 M ($NaCF_3SO_3$). The final concentrations of complex were between 0.01 and 0.02 M. The final solutions also contained CF_3SO_3H (0.6 M) and $Mn(CF_3SO_3)_2$ (0.1 M). Mn^{2+} was added in order to remove the large resonance line of bulk water by paramagnetic exchange broadening allowing observation of the bound water region (±100 ppm from bulk water).[32] The [H^+] used insured that the complexes were present in their triaqua forms. For the study on $[W_3(\mu_3\text{-}O)_2(\mu\text{-}CH_3CO_2)_6(OH_2)_3]^{2+}$ the samples were sealed under argon to prevent air oxidation at the prolonged high temperatures used. Oxygen-17 NMR spectra were recorded in standard thin walled 10-mm-o.d. tubes on a Bruker AM-300 instrument operating at 40.56 MHz. Spectra were recorded in the temperature range 15–80 °C over defined time intervals ranging between 158 s and 34 mins, depending upon the complex studied, using 15 000–100 000 transients accumulated over a sweep range of 62 500 Hz and a 90° pulse width of 27 μs. Rate constants were obtained by fitting the height of the bound water resonance (usually ~+80 ppm from bulk water) as a function of time to a standard exponential function. The temperature of the probe was calibrated using the ^1H NMR resonances of an ethylene glycol standard.

Other Reagents. Sodium triflate, $NaCF_3SO_3$, was prepared by neutralization of solutions of CF_3SO_3H (Fluorochem) with NaOH and recrystallization from water/ethanol. All other reagents, chemicals, and solvents were of reagent grade quality and were used as supplied. Double-distilled water was used throughout for the kinetic measurements.

Results

$[Mo_3(\mu_3\text{-}O)_2(\mu\text{-}CH_3CO_2)_6(OH_2)_3]^{2+}$. (a) NCS^- Complex Formation. Two stages of reaction were observed, the first generally complete within 6 h and the second requiring several days. These were assigned to substitution first by one then two NCS^- ligands. The absorbance–time data were analyzed by a consecutive reaction treatment involving extrapolation of the linear portion of ln ($A_{inf} - A_t$) versus t plots for the second stage back to t = 0 in order to obtain the A_{inf} value for the first stage. In this way pseudo-first-order rate constants for both stages could be determined. Plots of k_{obs} versus [NCS^-]/n for the two stages as a function of temperature are shown in Figures 5 and 6. Statistical factors (n) of 3 (for reaction on the triaqua complex) and 2 (reaction on the diaqua(thiocyanate) complex) have been applied on the basis of n identical Mo centers available to the incoming NCS^- ligand.[33] The plots for the first stage show evidence of saturation kinetic behavior in [NCS^-]. There are two possible interpretations of this behavior. The first is to consider the first step as being the reversible dissociation of a water ligand from the triaqua complex followed by reaction with NCS^- (D mechanism). The second is a consideration of ion-pair preassociation of the reactants followed by interchange (I mechanism). For reasons that will become clear below we favor the second option, Scheme I, which also takes into account the acidic nature of the coordinated water ligands,[34] $K_M \sim 1 \times 10^{-4}$ M (value (25 °C) estimated from the pH of known concentrations of $[Mo_3O_2(CH_3CO_2)_6(OH_2)_3]$-

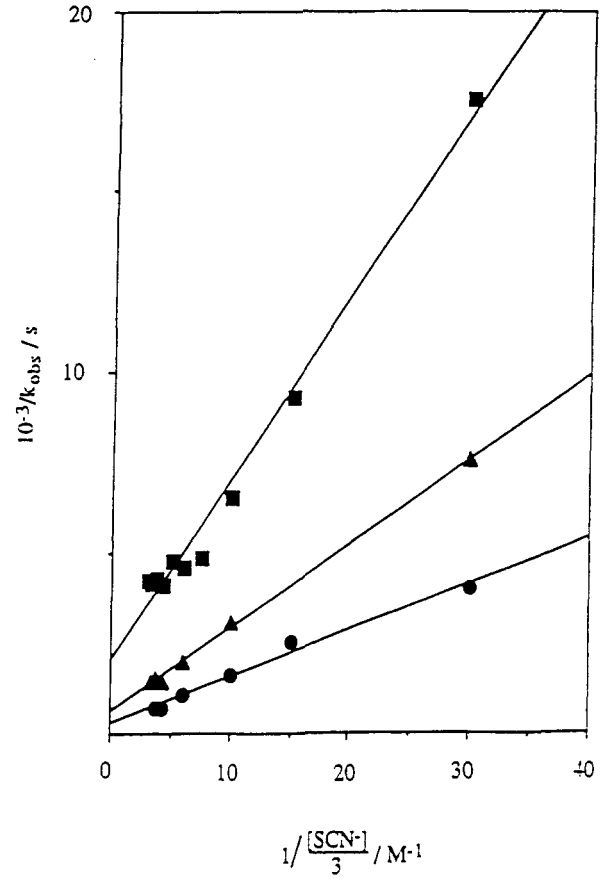

Figure 6. Plots of $1/k_{obs}$ (s) versus $1/[NCS^-]$ (M^{-1}) for the first stage of reaction of $[Mo_3(\mu_3\text{-}O)_2(\mu\text{-}CH_3CO_2)_6(OH_2)_3]^{2+}$ with NCS^-, pH 3.0, I = 1.0 M ($NaCF_3SO_3$): (■) 47 °C; (▲) 55 °C; (●) 60 °C.

Scheme I

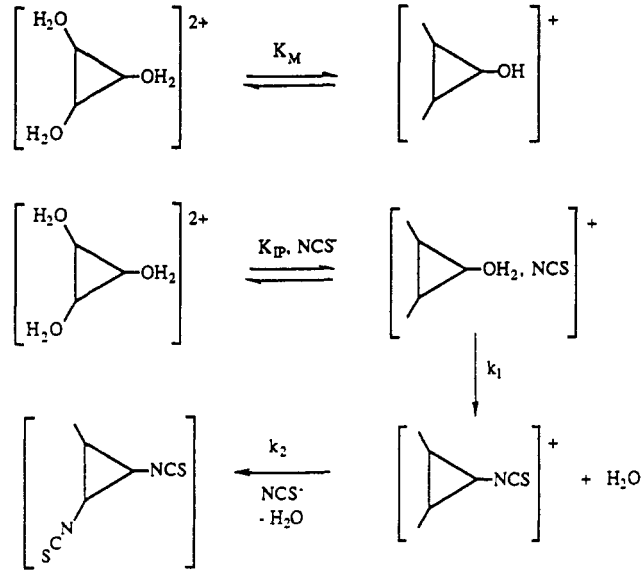

(32) Hugi-Cleary, D.; Helm, L.; Merbach, A. E. *J. Am. Chem. Soc.* **1987**, *109*, 4444.

(33) Vanderheiden, D. B.; King, E. L. *J. Am. Chem. Soc.* **1973**, *95*, 3860. Kathirgamanathan, P.; Soares, A. B.; Richens, D. T.; Sykes, A. G. *Inorg. Chem.* **1985**, *24*, 1313.

(34) Bino, A.; Gibson, D. *Inorg. Chem.* **1984**, *23*, 109.

Table I. Kinetic Data for the Reaction of $[Mo_3(\mu_3\text{-}O)_2(\mu\text{-}CH_3CO_2)_6(OH_2)_3]^{2+}$ with NCS^-, pH 3.0, I = 1.0 M ($NaCF_3SO_3$)

First Stage

T/°C	$10^4k_1/s^{-1}$	K_{IP}/M
47.0	4.96	1.5
55.0	18.61	0.9
60.0	40.45	0.7

$\Delta H^{\ddagger}_1 = 140 \pm 0.9$ kJ mol^{-1} $\Delta H^{\circ}_{IP} = -52.4 \pm 2.7$ kJ mol^{-1}
$\Delta S^{\ddagger}_1 = +130 \pm 2.7$ J K^{-1} mol^{-1} $\Delta S^{\circ}_{IP} = -160.4 \pm 8.2$ J K^{-1} mol^{-1}

Second Stage

T/°C	$10^5k_2/s^{-1}$	
47.0	9.34	$\Delta H^{\ddagger}_2 = 120.1 \pm 0.6$ kJ mol^{-1}
55.0	28.94	$\Delta S^{\ddagger}_2 = +52.6 \pm 1.7$ J K^{-1} mol^{-1}
60.0	56.42	

$(ClO_4)_2$ in CO_2-free distilled water and by subsequent titration with standard NaOH). It follows from the scheme that if $K_M \sim [H^+]$ then k_{obs} for the first stage is given by (1). (1) can be

$$k_{obs} = \frac{(k_1/3)K_{IP}[NCS^-][H^+]}{([H^+] + K_M)(1 + K_{IP}[NCS^-]/3)} \quad (1)$$

rearranged into the double reciprocal relationship (2) and

$$\frac{1}{k_{obs}} = \frac{3([H^+] + K_M)}{k_1K_{IP}[NCS^-][H^+]} + \frac{([H^+] + K_M)}{k_1[H^+]} \quad (2)$$

consistent with this plots of $1/k_{obs}$ versus $1/[NCS^-]$ plots are linear for the three temperatures studied, Figure 6, with intercept $([H^+] + K_M)/k_1[H^+]$, hence k_1 and slope $3([H^+] + K_M)/k_1K_{IP}[H^+]$ from which the ratio of intercept to slope gives K_{IP}. A temperature independent value for K_M of 1×10^{-4} M was assumed (see below). Values of k_1 and K_{IP} so obtained along with their corresponding activation and thermodynamic parameters are listed in Table I. (A pH variation study was not possible since a suitable buffer could not be found which did not interfere with the reaction. For example use of acetate buffer caused a marked retardation presumably due to strong ion-pair association of acetate perhaps involving hydrogen-bonding with the water ligands.)

For the second stage of reaction, simple linear plots passing through the origin were observed for each temperature allowing bimolecular rate constants to be obtained from the slopes. These are also listed also in Table I.

(b) Oxalate Complex Formation. The reaction with oxalate shows only a small bathochromic shift in the visible maxima of the Mo_3 complex accompanied by a small rise in absorbance. This is consistent with replacement of one O-donor ligand (H_2O) with another (oxalate) and the position of oxalate in the spectrochemical series. There were uncertainties as to the final absorbance readings in some cases due to a small steady decrease. For this reason A_{inf} values were estimated using the method of Swinbourne.[35] Such plots were found to be linear up to 3 half-lives for Δt values over at least 1 half-life. For the range of oxalate concentrations studied (0.01–0.05 M) the dependence upon $[oxalate]_T$ was linear passing through a clear intercept. Figure 7 shows representative plots for runs at 40 °C at different pH values (adjusted with CF_3SO_3H). This behavior is suggestive of equilibration kinetics. In the absence of a discernable second stage of reaction a statistical factor of 3 was assumed (3) with

$$k_{obs} = (k_f/3)[oxalate]_T + k_b \quad (3)$$

k_f and k_b representing the forward and reverse rate constants

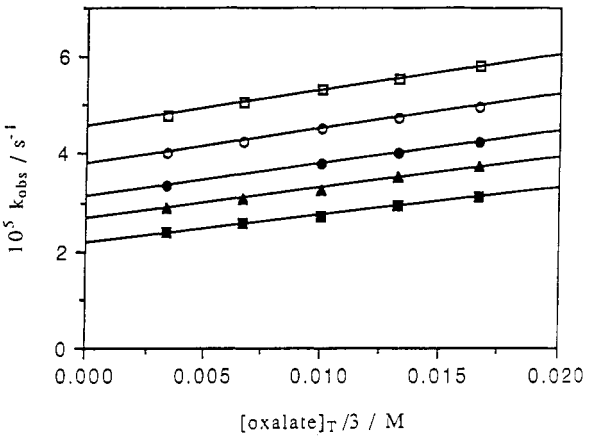

Figure 7. Plots of k_{obs} (s^{-1}) versus $[oxalate]_T$ (M) for the reaction of $[Mo_3(\mu_3\text{-}O)_2(\mu\text{-}CH_3CO_2)_6(OH_2)_3]^{2+}$ with oxalate as a function of pH, T = 40 °C, I = 1.0 M ($NaCF_3SO_3$): (■) pH 2.78; (▲) pH 3.09; (●) pH 3.36; (○) pH 3.56; (□) pH 3.89.

respectively. The slopes and intercepts of Figure 7 both show an increase with increasing pH so a consideration of the $[H^+]$ dependence of the reaction was appropriate. Oxalic acid undergoes two successive acid dissociations (eqs 4 and 5). Values

$$H_2C_2O_4 \overset{K_{ox1}}{\rightleftharpoons} HC_2O_4^- + H^+ \quad (4)$$

$$HC_2O_4^- \overset{K_{ox2}}{\rightleftharpoons} C_2O_4^{2-} + H^+ \quad (5)$$

for K_{ox1} and K_{ox2} as a function of temperature have been determined by several workers at ionic strength 1.0 M.[36-38] At 25 °C the values are $K_{ox1} = 8.4 \times 10^{-2}$ M and $K_{ox2} = 2.8 \times 10^{-4}$ M. In the pH range of study (2.5–3.9) amounts of the fully protonated form $H_2C_2O_4$ may be neglected and the total oxalate concentration can be represented by (6). The increase in k_{obs}

$$[oxalate]_T = [HC_2O_4^-] + [C_2O_4^{2-}] \quad (6)$$

values with decreasing $[H^+]$ initially suggested that the dianion, $C_2O_4^{2-}$ was either the dominant reactant or reacted at a much faster rate that the monoanion, $HC_2O_4^-$. In the pH range studied, participation of the monohydroxy form of the trimer was also a possibility. Subsequent plots of k_f vs $[H^+]^{-1}$ and k_f^{-1} vs $[H^+]$ were curved indicating that the relevant rate law contained terms other than that representing simple reaction of $C_2O_4^{2-}$ with the triaqua complex. Further fits involved participation of both oxalate anions in parallel reactions with the triaqua complex and eventually the data was fitted to a mechanism wherein relevant concentrations of the monohydroxy complex was also considered cf NCS^- study. The $[H^+]$ dependence of k_f was found to be consistent with the mechanism shown in Scheme II, wherein $[Mo_3O_2(CH_3CO_2)_6(OH_2)_3]^{2+}$ was written as Mo_3^{2+} for the sake of simplicity and the expression for k_f was of the form shown in (7). Consistent with (7) subsequent plots of $k_f([H^+] +$

$$k_f = \frac{k_1[H^+]^2 + k_2K_{ox2}[H^+]}{([H^+] + K_M)([H^+] + K_{ox2})} \quad (7)$$

$K_M)([H^+] + K_{ox2})/[H^+]$ versus $[H^+]$ were linear for the three temperatures studied, Figure 8. Values of k_1 and k_2 were computed as a function of temperature from the slopes and intercepts respectively of Figure 8 using calculated values of K_{ox2} as a function of temperature. These are listed in Table II. As

(35) Swinbourne, E. S. *J. Chem. Soc.* **1960**, 2371.

(36) Davies, G.; Watkins, K. O. *Inorg. Chem.* **1970**, *9*, 2735.
(37) Nor, O.; Sykes, A. G. *J. Chem. Soc., Dalton Trans.* **1973**, 1232.
(38) Moorhead, E. G.; Sutin, N. *Inorg. Chem.* **1966**, *5*, 1866.

Scheme II

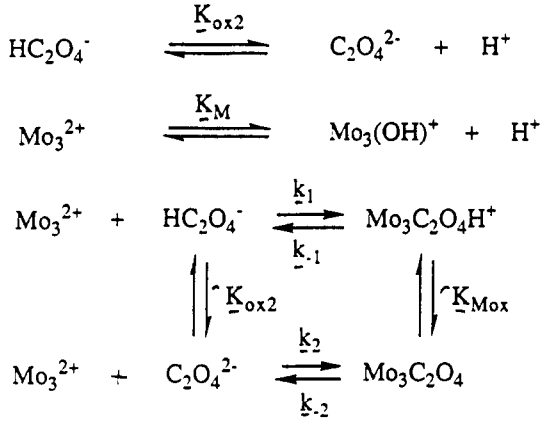

Table II. Kinetic Data for the Reaction of $[Mo_3(\mu_3\text{-}O)_2(\mu\text{-}CH_3CO_2)_6(OH_2)_3]^{2+}$ with Oxalate, I = 1.0 M ($NaCF_3SO_3$)

Forward (Complexation) Reaction

T/°C	$10^4k_1/M^{-1}\ s^{-1}$	$10^3k_2/M^{-1}\ s^{-1}$	$10^4K_{ox2}/M^a$
40.0	4.08	1.67	2.61
47.0	7.95	5.36	2.54
55.0	16.29	14.47	2.45

$\Delta H^{\ddagger}_1$ = 76.2 ± 0.3 kJ mol^{-1} $\Delta H^{\ddagger}_2$ = 120 ± 8.6 kJ mol^{-1}
$\Delta S^{\ddagger}_1$ = −67.0 ± 0.9 J K^{-1} mol^{-1} $\Delta S^{\ddagger}_2$ = +85.0 ± 26.8 J K^{-1} mol^{-1}

Backward (Aquation) Reaction

T/°C	$10^5k_{-1}/M^{-1}\ s^{-1}$	$10^5k_{-2}/M^{-1}\ s^{-1}$
40.0	1.40	5.30
47.0	2.50	14.10
55.0	12.20	48.60

$\Delta H^{\ddagger}_{-1}$ = 121.4 ● 30.0 kJ mol^{-1} $\Delta H^{\ddagger}_{-2}$ = 123.7 ± 5.4 kJ mol^{-1}
$\Delta S^{\ddagger}_{-1}$ = +48.0 ± 93.6 J K^{-1} mol^{-1} $\Delta S^{\ddagger}_{-2}$ = +67.5 ± 16.8 J K^{-1} mol^{-1}

[a] Calculated from literature values of ΔH°_{ox2} and ΔS°_{ox2} at I = 1.0 M.

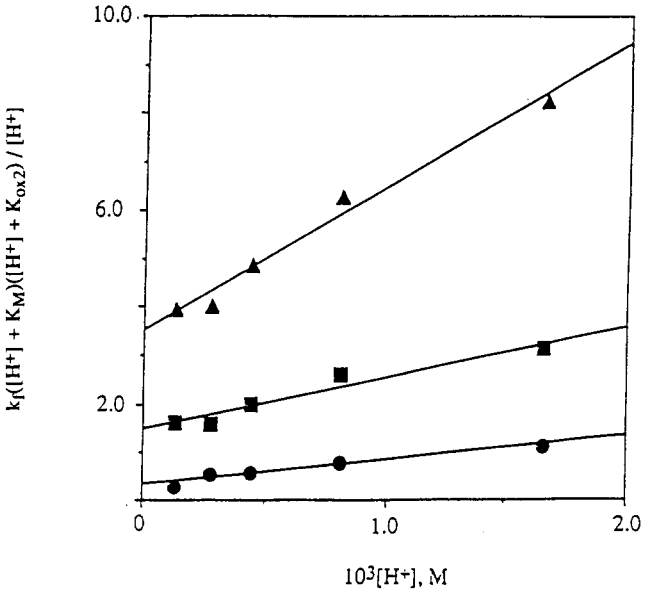

Figure 8. Linear plots of $k_f([H^+] + K_M)([H^+] + K_{ox2})/[H^+]$ versus $[H^+]$ a different temperatures for the reaction of $[Mo_3(\mu_3\text{-}O)_2(\mu\text{-}CH_3CO_2)_6(OH_2)_3]^{2+}$ with oxalate at I = 1.0 M ($NaCF_3SO_3$): (●) 40 °C; (bsd) 47 °C; (▲) 55 °C.

in the NCS^- study a temperature independent K_M value of ~1 × 10^{-4} M was initially assumed for the purpose of constructing the linear plots in Figure 8. A nonlinear least-squares fit to (7) gave rise to iterated values for K_M respectively as (4.36 ± 2.60) × 10^{-5} M (40 °C) and (7.00 ± 1.34) × 10^{-5} M (55 °C) in addition to values for k_1 and k_2 similar to those in Table II. The kinetic values for K_M, in being close to the value estimated by pH titration, provide further support for the proposed mechanism.

The $[H^+]$ dependence of the reverse reaction rate constant, k_b, on the basis of Scheme II would be of the form shown in (8) and

$$k_b = \frac{k_{-1}[H^+] + k_{-2}K_{Mox}}{([H^+] + K_{Mox})} \quad (8)$$

consistent with this plots of $k_b([H^+] + K_{Mox})$ versus $[H^+]$ were linear for all three temperatures assuming a K_{Mox} of 4 × 10^{-4} M. It would be expected that K_{Mox} should not be very different from the second acid dissociation constant of oxalic acid, K_{ox2}. Values of k_{-1} and k_{-2} so determined are also listed in Table II along with their activation parameters. A nonlinear least-squares fit to (8), assuming 4 × 10^{-4} M as an initial estimate for K_{Mox}, gave rise to iterated values for K_{Mox} respectively as (2.31 ± 0.58) × 10^{-4} M (40 °C) and (2.80 ± 0.49) × 10^{-4} M (55 °C) along with values of k_{-1} and k_{-2} similar to those in Table II.

$[W_3(\mu_3\text{-}O)_2(\mu\text{-}CH_3CO_2)_6(OH_2)_3]^{2+}$. Oxalate Complex Formation. Spectral changes in the UV–visible region of the dioxo-capped W complex showed a slight shift in the 450-nm band maximum to lower energy accompanied by loss of the 370-nm peak to give a shoulder resulting from a marked increase in absorbance below 350 nm. These observations, as with the Mo complex, are consistent with substitution of the water ligands by oxalate. Reactions were followed at 55 °C and at pH 3.83 for comparison with the bicapped Mo complex. Equilibration kinetics representing a single stage of reaction were observed, as in the Mo_3 complex, with values of k_f and k_b (55 °C) being respectively (2.76 ± 0.17) × 10^{-4} M^{-1} s^{-1} and (9.84 ± 0.19) × 10^{-6} s^{-1}. A statistical factor of 3 was applied.

$[W_3(\mu_3\text{-}O)(\mu\text{-}CH_3CO_2)_6(OH_2)_3]^{2+}$. $[NCS^-]$ Complex Formation. A single kinetic stage was observed with k_{obs} values found from the slopes of ln $(A_t - A_{int})$ vs t plots linear to greater than 4 half-lives. Isosbestic points were observed at ~745, 580, 550, and 480 nm, which become ultimately lost in the latter stages of reaction due presumably to an instability in the final thiocyanato complex on prolonged heating. Values of k_{obs}/s^{-1}, as a function of $[NCS^-]$, were found to obey (9) with no evidence of saturation

$$k_{obs} = (k_1/3)[NCS^-] \quad (9)$$

kinetics. A statistical factor of 3 was again applied for reaction at the three identical tungsten sites. At 50 °C, pH 2.0 the value of k_1 was evaluated as 2.4 × 10^{-4} M^{-1} s^{-1}.

Water Exchange. A typical plot of height of the ^{17}O NMR resonance of coordinated water versus time for the monocapped complex $[W_3(\mu_3\text{-}O)(\mu\text{-}CH_3CO_2)_6(OH_2)_3]^{2+}$ at $[H^+]$ 0.6 M, I = 1.0 M ($NaCF_3SO_3$), is shown in Figure 9, the solid line being the fit to a standard exponential function. Table III lists the results of variable temperature kinetic studies carried out respectively on the three complexes.

Discussion

NCS^- complexation on $[Mo_3(\mu_3\text{-}O)_2(\mu\text{-}CH_3CO_2)_6(OH_2)_3]^{2+}$ shows two stages of reaction which are believed to represent stepwise substitution of one and then two H_2O ligands by NCS^-. The first stage shows saturation kinetic behavior. Of the two possible explanations for this we favor an ion-pair interchange mechanism on the basis of the following findings. First, the K_{IP}, ΔH°_{IP} and ΔS°_{IP} values so determined are typical of those expected for 2+/1− charged reactants at ionic strength 1.0 M.[39-41] Secondly, the lack of similar saturation kinetics for the second

(39) Burgess, J. *Metal Ions in Solution.* Ellis Horwood: Chichester, England, 1977; p 353 and references therein.
(40) Eisenstadt, M. *J. Chem. Phys.* **1969**, *51*, 4421.
(41) Nancollas, G. H.; Sutin, N. *Inorg. Chem.* **1964**, *3*, 360.

Table III. Kinetic Parameters for Water Exchange on $[M_3(\mu_3\text{-}O)_2(\mu\text{-}CH_3CO_2)_6(OH_2)_3]^{2+}$ (M = Mo, W) and $[W_3(\mu_3\text{-}O)(\mu\text{-}CH_3CO_2)_6(OH_2)_3]^{2+}$, $[H^+]$ = 0.6 M, I = 1.0 M ($NaCF_3SO_3$)

complex	T/°C	10^4k_{ex}/s^{-1}	$\Delta H^{\ddagger}_{ex}$/kJ mol^{-1}	$\Delta S^{\ddagger}_{ex}$/J K^{-1} mol^{-1}
$[Mo_3O_2(CH_3CO_2)_6(OH_2)_3]^{2+}$	37.0	0.38 ± 0.04	125.8 ± 9.6	76.6 ± 30.0
	43.5	1.14 ± 0.21		
	50.0	3.77 ± 0.30		
	59.0	9.84 ± 0.51		
$[W_3O_2(CH_3CO_2)_6(OH_2)_3]^{2+}$	53.5	0.09 ± 0.01	58.30 ± 8.39	−164.3 ± 24.9
	64.5	0.16 ± 0.01		
	76.0	0.38 ± 0.01		
$[W_3O(CH_3CO_2)_6(OH_2)_3]^{2+}$	4.5	0.97 ± 0.06	52.69 ± 3.27	−130.6 ± 11.2
	13.5	2.46 ● 0.12		
	25.0	5.54 ± 0.36		
	33.0	9.15 ± 0.94		

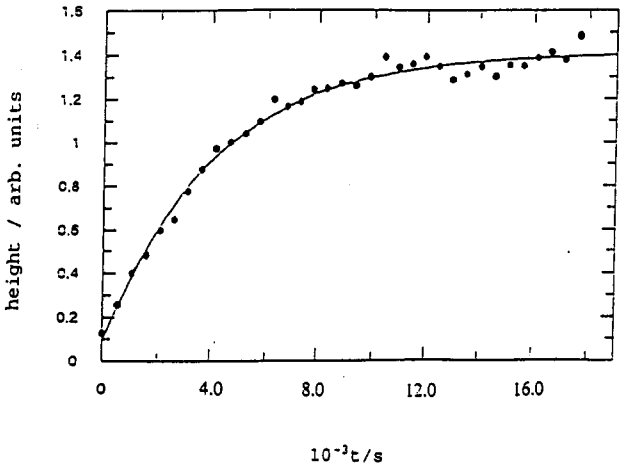

Figure 9. Height of the ^{17}O NMR resonance of bound water on $[W_3(\mu_3\text{-}O)(\mu\text{-}CH_3CO_2)_6(OH_2)_3]^{2+}$ (0.02M) plotted as a function of time following mixing with 10 atom % H_2 ^{17}O at $[H^+]$ = 0.6 M, $[Mn^{2+}]$ = 0.1 M, and I = 1.0M ($NaCF_3SO_3$). The solid line is a fit to a standard exponential function.

stage would be difficult to explain if a general D mechanism was relevant for this complex. Extrapolated rate constants (25 °C) for the interchange step of the first stage (9.4×10^{-6} s^{-1}) and water exchange (5.6×10^{-6} s^{-1}) are comparable. This observation coupled with large $\Delta H^{\ddagger}$ and positive $\Delta S^{\ddagger}$ values characterizing both processes suggests that the mechanism is probably I_d. (A rate constant of 1.1×10^{-5} s^{-1} (45 °C) reported for presumably the first stage of substitution of water by CD_3OD is comparable with those obtained in the present study and provides additional support for the I_d mechanism.)[30]

These rate constants are much smaller however than those (25 °C) characterizing similar processes on e.g. $[Mo_3O_4(OH_2)_9]^{4+}$.[18,26] Most notably, the water exchange rate constant (25 °C) for $[Mo_3(\mu_3\text{-}O)_2(\mu\text{-}CH_3CO_2)_6(OH_2)_3]^{2+}$ is some 8 orders of magnitude smaller than that for the more labile d-H_2O on $[Mo_3O_4(OH_2)_9]^{4+}$,[18] a feature that is now believed to reflect the importance of the conjugate-base-assisted pathway in the latter via deprotonation at an adjacent water ligand.[25] An additional factor in the acetato-bridged complexes would be the greater steric hindrance provided by the acetate ligands themselves toward approach of the incoming terminal ligand. Together with the extremely large $\Delta H^{\ddagger}$ values, this would suggest an I_d process tending toward the dissociative limit for loss of a water ligand.

For the second stage of NCS^- complexation on $[Mo_3(\mu_3\text{-}O)_2(\mu\text{-}CH_3CO_2)_6(OH_2)_3]^{2+}$, the absence of saturation behavior is believed to reflect the much smaller K_{IP} value expected for a 1+/1− reactant pair. The 10× smaller k_{obs} values observed for the second stage could thus be merely a reflection of the lower K_{IP} values leading conceivably to rate constants for the interchange step not dissimilar to those for the first stage. Correspondingly the absence of a discernable third stage of reaction may be explained as reflecting an even smaller value of K_{IP}. Almost identical rate constants (within a factor of 2) are known to

Scheme III

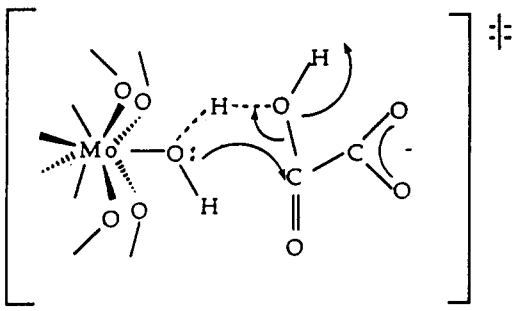

characterize the three successive stages of CD_3OD substitution for water on the complexes $[Mo_3(\mu_3\text{-}CCH_3)(\mu_3\text{-}O)(\mu\text{-}CH_3CO_2)_6(OH_2)_3]^+$ and $[W_3(\mu_3\text{-}O)(\mu\text{-}CH_3CO_2)_6(OH_2)_3]^{2+}$.[30]

Complexation by oxalate however appears to involve a somewhat different process wherein both $HC_2O_4^-$ and $C_2O_4^{2-}$ (both relevant to the pH range studied) are involved in an equilibration reaction with the triaqua complex. The absence of saturation kinetics reflects the low oxalate concentration range used due to limits in solubility. The most striking feature however is the markedly differing activation parameters characterizing reaction with the two oxalate anions. For $HC_2O_4^-$, the value of $\Delta H^{\ddagger}$ (76 kJ mol^{-1}) is significantly smaller than those characterizing water exchange (126 kJ mol^{-1}) and NCS^- complexation (141 kJ mol^{-1}) and is, together with the noticably negative $\Delta S^{\ddagger}$ (−67 J K^{-1} mol^{-1}), reminiscent of the values obtained by van Eldik and Harris[42] for complexation by both $H_2C_2O_4$ and $HC_2O_4^-$ on $[Co(NH_3)_5(OH_2)]^{3+}$. Jordan and Taube[43] had earlier proposed C–O bond breaking as the predominant mechanism for the acid catalyzed aquation of $[Co(NH_3)_5(HC_2O_4)]^{2+}$, and this led to the proposal of a similar mechanism for the reverse complexation process.[42] Conceivably such a mechanism cannot be ruled out here wherein complexation by $HC_2O_4^-$ takes place via a concerted process (Scheme III): involving release of a water ligand via C–O (oxalate) rather than Mo–OH_2 bond breakage. Such a mechanism is now believed to become important for oxalate complexation reactions on aquametal complexes when the rate of the concerted C–O bond breakage process exceeds that of water exchange on the metal center[44,45] as it does here.

Complexation by $C_2O_4^{2-}$ on $[Mo_3(\mu_3\text{-}O)_2(\mu\text{-}CH_3CO_2)_6(OH_2)_3]^{2+}$ is more difficult to evaluate owing to the so-called proton ambiguity problem. Conceivably the reactants could be either Mo_3^{2+} with $C_2O_4^{2-}$ or $Mo_3(OH)^+$ with $HC_2O_4^-$ or a combination of both, the similar acid dissociation constants linking each ($\sim 10^{-4}$ M) rendering all four possible reactants relevant in the pH range studied (2.5–3.9). Consideration of the sole involvement of Mo_3^{2+} with $C_2O_4^{2-}$ gives a bimolecular rate

(42) van-Eldik, R.; Harris, G. M. *Inorg. Chem.* **1978**, *14*, 10.
(43) Andrade, C.; Jordan, R. B.; Taube, H. *Inorg. Chem.* **1970**, *9*, 711.
(44) Patel, A.; Leitch, P.; Richens, D. T. *J. Chem. Soc., Dalton Trans.* **1991**, 1029.
(45) McMahon, M. R.; McKenzie, A.; Richens, D. T. *J. Chem. Soc., Dalton Trans.* **1988**, 711.

Table IV. Summary of Kinetic Parameters for Water Exchange and Complex Formation on Trinuclear Acetato-Bridged Cluster Complexes of Molybdenum and Tungsten

complex	incoming ligand	k_{298}/M^{-1} s^{-1}	$\Delta H^{\ddagger}$/kJ mol^{-1}	$\Delta S^{\ddagger}$/J K^{-1} mol^{-1}	mechanism	ref
$[Mo_3O_2(OAc)_6(OH_2)_3]^{2+}$	H_2O	5.6×10^{-6} [a]	126	+77	I_D	this work
	SCN^-	9.4×10^{-6} [a]	141	+131	I_D	this work
	$C_2O_4^{2-}$	$\sim 8 \times 10^{-6}$ [a]	120	+85	I_D	this work
	$HC_2O_4^-$	8.94×10^{-5}	76	−67	"concerted"	this work
	CD_3OD	1.1×10^{-5} [b]			I_D	30
$[Mo_3O(CCH_3)(OAc)_6(OH_2)_3]^+$	CD_3OD	1.2[b]	93	+49	I_D or D	30
$[Mo_3O(CCH_3)(OAc)_6(py)_3]^{2+}$	py-d_5	8.6×10^{-4} [c]	112	+77	D	30
$[W_3O_2(OAc)_6(OH_2)_3]^{2+}$	H_2O	1.02×10^{-6} [a]	58	−164	I_A or A?	this work
	CD_3OD	$<5 \times 10^{-7}$ [b]				30
$[W_3O(OAc)_6(OH_2)_3]^{2+}$	H_2O	5.3×10^{-4} [a]	53	−131	I_A or A?	this work
	SCN^-	1.5×10^{-4} [f]			I_A	this work
	CD_3OD	5.5×10^{-5} [g]	113	+56	I_D or D	30

[a] s^{-1}, I = 1.0 M ($NaCF_3SO_3$). [b] s^{-1}, 44.8 °C in neat CD_3OD. [c] s^{-1} in CD_3NO_2 containing py-d_5. [d] s^{-1} at 50 °C. [e] s^{-1} (k_1) at 55 °C, I = 1.0 M ($NaCF_3SO_3$). [f] s^{-1} (k_1) at 50 °C, I = 1.0 M ($NaCF_3SO_3$). [g] s^{-1} at 24.5 °C in neat CD_3OD.

constant (25 °C) of 1.64×10^{-4} M^{-1} s^{-1}. Consideration of an ion-pair interchange mechanism would require an estimate for K_{IP}. Such a value for 2+/2− reactant pairs are normally in the range 10–20 M^{-1}.[39] If a value of ~20 M^{-1} is assumed, then the interchange rate constant for Mo_3^{2+} reacting with $C_2O_4^{2-}$ would be $\sim 8 \times 10^{-6}$ s^{-1}, which is now very close to the values for water exchange and NCS^- complexation. The associated values of $\Delta H^{\ddagger}$ (120 kJ mol^{-1}) and $\Delta S^{\ddagger}$ (+85 J K^{-1} mol^{-1}) are also reminiscent of those for water exchange, implying that the mechanism here is I_d.

Consideration of the other extreme situation, $Mo_3(OH)^+$ reacting with $HC_2O_4^-$, would lead to (7) being rearranged as (10). If K_M is assumed to have a temperature independent value

$$k_f = \frac{k_1[H^+]^2 + k_3K_M[H^+]}{([H^+] + K_M)([H^+] + K_{ox2})} \qquad (10)$$

of 1×10^{-4} M as before then values of k_3 (M^{-1} s^{-1}) respectively at 40, 47, and 55 °C are 4×10^{-3}, 14×10^{-3}, and 36×10^{-3} giving rise to k_3(25 °C) = 5×10^{-4} M^{-1} s^{-1}, $\Delta H^{\ddagger}$ = 116 kJ mol^{-1}, and $\Delta S^{\ddagger}$ = +81 J K^{-1} mol^{-1}. These activation parameters would seem to be inconsistent with the kind of concerted mechanism assigned to the reaction of Mo_3^{2+} with $HC_2O_4^-$, and thus it is tentatively concluded that within the limiting constraints of the proton ambiguity the mechanism for the second path involves reaction of the triaqua complex with $C_2O_4^{2-}$ in an I_d process.

Aquation of the Mo_3–C_2O_4 complex is more favored on the basis of 5× larger k_{-2} values than k_{-1} at each temperature. This is somewhat surprising since both the rate constants and activation parameters for k_{-2} favor the same I_d process as for the forward reaction and not attack of OH^- on the coordinated oxalate (reverse of k_1 path). Direct attack by OH^- on the metal would seem unlikely on steric grounds. Perhaps monodentate coordination of $C_2O_4^{2-}$ is less favored in that it would probably prefer to be chelated (not possible here). An additional factor for the coordinated dianion might be a greater electrostatic repulsion from the proximal bridging acetate groups.

Oxalate complexation has also been studied at 55 °C, pH 3.83, on $[W_3(\mu_3\text{-}O)_2(\mu\text{-}CH_3CO_2)_6(OH_2)_3]^{2+}$ for comparison with molybdenum. Equilibration kinetics were again observed with k_f and k_b values respectively at 55 °C being $(2.76 \pm 0.17) \times 10^{-4}$ M^{-1} s^{-1} and $(9.84 \pm 0.19) \times 10^{-6}$ s^{-1}, these values being ~20× and ~40× smaller, respectively, than those for Mo_3^{2+} under the same conditions. Rate constants ~20× smaller also characterize the kinetics of terminal water substitution on $[W_3(\mu_3\text{-}X)(\mu\text{-}X)_3(OH_2)_9]^{4+}$ (X = O, S) versus the Mo_3 analogues for which an I_d mechanism is indicated. The increased inertness in the 5d element compounds is a phenomenon believed to relate to the so-called relativistic expansion effect[46] which results in increased 5d orbital participation and, as a result, stronger W–W and W–L bonds. The latter is important therefore when considering dissociatively activated mechanisms. We tentatively conclude that the more inert behavior of $[W_3(\mu_3\text{-}O)_2(\mu\text{-}CH_3CO_2)_6(OH_2)_3]^{2+}$ here, versus its Mo_3 analogue, is due to a retardation in the rate for the I_d pathway governing reaction with $C_2O_4^{2-}$ (the rate for the concerted k_1 pathway assumed to be independent of the metal).[44,45]

The rate constant, k_1(50 °C) = 2.4×10^{-4} M^{-1} s^{-1}, for NCS^- complexation on the monooxo-capped complex $[W_3(\mu_3\text{-}O)_2(\mu\text{-}CH_3CO_2)_6(OH_2)_3]^{2+}$ is similar in magnitude to that for the forward reaction with oxalate on the dioxo-capped W complex, k_f(55 °C) = 2.76×10^{-4} M^{-1} s^{-1}. However such a direct comparison is difficult and moreover misleading due to the presence of competing parallel reaction pathways in the oxalate complexation reaction. For a meaningful consideration of the intrinsic reactivity of each complex, it is now appropriate to consider the rates for the various complexation reactions with those for water exchange, Table IV.

The kinetic data characterizing water exchange on $[Mo_3(\mu_3\text{-}O)_2(\mu\text{-}CH_3CO_2)_6(OH_2)_3]^{2+}$ are in support of the proposed I_d mechanism. Since $[W_3(\mu_3\text{-}O)_2(\mu\text{-}CH_3CO_2)_6(OH_2)_3]^{2+}$ shows more inert behavior in complex-forming reactions, one might expect activation parameters for water exchange similar to those on molybdenum, perhaps a slightly larger $\Delta H^{\ddagger}$. However this was surprisingly not the case. A much smaller $\Delta H^{\ddagger}$ value (58 kJ mol^{-1}) and markedly negative $\Delta S^{\ddagger}$ value (−164 J K^{-1} mol^{-1}) characterized water exchange on $[W_3(\mu_3\text{-}O)_2(\mu\text{-}CH_3CO_2)_6(OH_2)_3]^{2+}$ such that at 25 °C the extrapolated rate constant for tungsten (1.02×10^{-6} s^{-1}) was only about one-fifth that for molybdenum. Such activation parameters are more typical of associatively activated processes.[47] A similarly low $\Delta H^{\ddagger}$ value (53 kJ mol^{-1}) and markedly negative $\Delta S^{\ddagger}$ value (−130 J K^{-1} mol^{-1}) also characterized water exchange on the corresponding monooxo-capped tungsten complex $[W_3(\mu_3\text{-}O)(\mu\text{-}CH_3CO_2)_6(OH_2)_3]^{2+}$ although here the rate constant at 25 °C (5.5×10^{-4} s^{-1}) is 500× larger than that on the dioxo-capped tungsten analogue. The absence of saturation kinetics for NCS^- complexation on $[W_3(\mu_3\text{-}O)(\mu\text{-}CH_3CO_2)_6(OH_2)_3]^{2+}$ suggests either that ion-pairing is less important for the incoming thiocyanate ligand or that an associative mechanism may be relevant. The lack of detectable ion-pairing could also conceivably reflect a significantly lower cationic charge at the reacting metal center, perhaps W(III), in this mixed-valence complex. For water exchange reactions following an I_a mechanism, a second-order rate constant can be derived as $3k_{ex}/55.56$ (M^{-1} s^{-1}) for reaction at three equivalent water ligands. For $[W_3(\mu_3\text{-}O)(\mu\text{-}CH_3CO_2)_6(OH_2)_3]^{2+}$, the extrapolated value at 50 °C is 1.6×10^{-4} M^{-1} s^{-1}, which may be compared with the rate constant (50 °C)

(46) (a) Pykko, P.; Desclaux, J. P. *Acc. Chem. Res.* **1979**, *12*, 276. (b) McKelvey, D. R. *J. Chem. Educ.* **1983**, *60*, 112.

(47) Wilkins, R. G. *The Kinetics and Mechanisms of Reactions of Transition Metal Complexes*, 2nd ed.; VCH: New York, 1991; pp 201–212 and references therein.

for bimolecular complex formation with NCS^-, $k_1 = 2.4 \times 10^{-4}$ M^{-1} s^{-1}. Such a rate constant for complex formation in excess of that for water exchange would however be in keeping with an associative mechanism.[47] On the other hand reported activation parameters for first stage of CD_3OD substitution of the water ligands on $[W_3(\mu_3\text{-}O)(\mu\text{-}CH_3CO_2)_6(OH_2)_3]^{2+}$ carried out in pure CD_3OD were $\Delta H^{\ddagger} = 113$ kJ mol^{-1} and $\Delta S^{\ddagger} = +56$ J K^{-1} mol^{-1}, more consistent with a dissociative process.[30] Also significantly the first order rate constant (25 °C) for CD_3OD substitution (5.5×10^{-5} s^{-1}) is 10× smaller than that for water exchange. Further work is therefore required in order to establish whether the apparent mechanistic changeover from I_d (D) (Mo) to I_a (A) (W) in these trinuclear carboxylato-bridged cluster complexes is unique to the water exchange process and not necessarily typical of the behavior of complex forming reactions. If verified it will represent the first such example of its kind. A further test for the existence of an associative mechanism on the tungsten complexes would be to measure the rate of Cl^- complexation. A k_{NCS}/k_{Cl} ratio well in excess of unity is now established as a good indicator of the presence of an associative activation process.[48] It is also hoped that variable pressure kinetic studies, presently in progress, will be able to provide a further insight.

Acknowledgment. We wish to thank the University of St. Andrews and Berco Ltd, Bermuda, for the award of a Sir James Irvine Scholarship to G.P. and the SERC for an allocation of fast atom bombardment mass spectral time on the National Service at the University of Swansea.

Supplementary Material Available: Tables of first order rate constants for the reactions of NCS^- and oxalate with $[Mo_3(\mu_3\text{-}O)_2(\mu\text{-}CH_3CO_2)_6(OH_2)_3]^{2+}$ (4 pages). Ordering information is given on any current masthead page.

(48) Sasaki, Y.; Sykes, A. G. *J. Chem. Soc., Dalton Trans.* **1975**, 1048.